10

Particularities of Membrane Gas Separation Under Unsteady State Conditions

Igor N. Beckman[1,2], Maxim G. Shalygin[1] and Vladimir V. Tepliakov[1,2]
[1]*A.V.Topchiev Institute of Petrochemical Synthesis, Russian Academy of Sciences*
[2]*M.V.Lomonosov Moscow Sate University, Chemical Faculty*
Russia

1. Introduction

Membranes become the key component of modern separation technologies and allow exploring new opportunities and creating new molecular selective processes for purification, concentration and separation of liquids and gases (Baker, 2002, 2004). Particularly the development of new highly effective processes of gas separation with application of existing materials and membranes takes specific place. In present time special attention devotes to purification of gas and liquid waste streams from ecologically harmful and toxic substances such as greenhouse gases, VOCs and others. From the fundamental point of view the development on new highly effective processes of gas separation demands the investigation of mass transfer in the unsteady (kinetic) area of gas diffusion through a membrane. This approach allows in some cases to obtain much higher selectivity of separation (using the same membrane materials) compared to traditional process where steady state conditions are applied. First studies of membrane separation processes under unsteady state conditions have demonstrated both opportunities and problems of such approach (Beckman, 1993; Hwang & Kammermeyer, 1975; Paul, 1971).

It was shown that effective separation in unsteady membrane processes is possible if residence times of mixture components significantly differ from each other that is the rare situation in traditional polymeric materials but well known for liquid membranes with chemical absorbents (Shalygin et al., 2006). Nevertheless similar behavior is possible in polymeric membranes as well when functional groups which lead to partial or complete immobilization of diffusing molecules are introduced in polymer matrix. Moreover the functioning of live organisms is related with controllable mass transfer through cell membranes which "operate" in particular rhythms. For example scientific validation of unsteady gas transfer processes through membranes introduces particular interest for understanding of live organisms' breathing mechanisms.

It can be noticed that development of highly effective unsteady membrane separation processes is far from systematic understanding and practical evaluation. Therefore the evolution of investigations in this area will allow to accumulate new knowledge about unsteady gas separation processes which can be prototypes of new pulse membrane separation technologies.

Theoretical description of unsteady mass transfer of gases in membranes is presented in this work. Examples of binary gas mixture separation are considered for three cases of gas

concentration variation on membrane: step function, pulse function and harmonic function. Unsteady gas flow rates and unsteady separation factors are calculated for all cases. Amplitude-frequency, phase-frequency and amplitude-phase characteristics as well as Lissajous figures are calculated for harmonic functions. The comparison of mixture separation efficiency under steady and unsteady mass transfer conditions is carried out. Calculations were performed for oxygen-nitrogen and oxygen-xenon gas mixtures separation by membranes based on polyvinyltrimethylsilane and for CO_2 transfer in liquid membrane with chemical absorbent of CO_2.

2. Regimes of unsteady gas transfer in membranes

The basis for mathematical modeling was taken from (Crank, 1975; Beckman et. al, 1989, 1991, 1996). According to the tradition scheme the gas flux at output of membrane in permeation method is defined by 1st Fick's law:

$$J(t) = -DA \left. \frac{\partial C(x,t)}{\partial x} \right|_{x=H} \tag{1}$$

where J – gas flux through membrane, A – area of membrane, D – diffusivity coefficient, H – thickness of membrane, C – concentration of gas molecules inside of membrane, t – time of diffusion, x – coordinate.
After some transient period of time the flux is achieving the steady-state condition:

$$J_{SS} = ADS \frac{p_u - p_d}{H}, \tag{2}$$

where S – solubility coefficient of gas in polymer, p_u and p_d – partial pressure of gas in upstream and downstream, respectively. Usually $p_u >> p_d$ and the steady-state gas flux through membrane (J_{ss}) can be expressed as:

$$J_{SS} = ADS \frac{p_u}{H} = AP \frac{p_u}{H}, \tag{3}$$

where $P = DS$ is the permeability coefficient.
Three steady-state selectivity factors can be defined for understanding of consequent detailed analysis: general (on the permeability coefficients) α_{SS}, kinetic (on the diffusivity coefficients) α_D and thermodynamic (on the solubility coefficients) α_S. Ideal selectivity for a pair of gases is described by equation (4):

$$\alpha_{SS} = \frac{P_A}{P_B} = \frac{D_A S_A}{D_B S_B} = \alpha_D \alpha_S, \tag{4}$$

where P_A, P_B the permeability coefficients of gases A and B, respectively; D_A, D_B are the diffusivity coefficients; S_A, S_B are the solubility coefficients.

2.1 Step function variation of gas concentration in upstream

In traditional permeability method at the input membrane surface at given moment of time the step function variation of gas concentration (high partial gas pressure) is created and at

the output membrane surface the partial gas pressure is keeping close to zero during whole diffusion experiment. At the beginning the gas transfer is unsteady and then after definite time the steady-state gas transfer is achieved.

In the frames of "classical" diffusion mechanism (that is the diffusion obedient to Fick's law and the solubility – to Henry's law) the unsteady distribution of concentration of diffusing gas $C(x,t)$ across the flat membrane with thickness H, is determined by the 2nd Fick's law:

$$\frac{\partial C(x,t)}{\partial t} = D\frac{\partial^2 C(x,t)}{\partial x^2} \tag{5}$$

Standard initial and boundary conditions are: $C(0,t)=C_u$; $C(H,t)=0$; $C(x,0)=0$, where C_u is the concentration of gas in membrane respected to partial pressure of gas at the upstream side in accordance with Henry's law:

$$C_u = Sp_u\,, \tag{6}$$

where S is solubility coefficient of gas in polymer.

The unsteady gas flux through membrane follows from the solution of Eq. (5) and can be expressed in two forms:

$$J(t) = J_{ss}\frac{4}{\sqrt{\pi}}\sqrt{\frac{H^2}{4Dt}}\sum_{m=0}^{\infty}\left\{-\frac{(2m+1)^2 H^2}{4Dt}\right\} \tag{7}$$

$$J(t) = J_{ss}\left[1+2\sum_{n=1}^{\infty}(-1)^n \exp\left\{-\left(\frac{n\pi}{H}\right)^2 Dt\right\}\right], \tag{7'}$$

where $J_{SS} = \frac{DC_u A}{H} = \frac{PAp_u}{H}$ is steady-state gas flux.

The series of the Eq. (7) is converged at small values of time and the series of the Eq. (7′) is converged at high values of time.

Traditionally, membrane gas transfer parameters P, D and S can be found from two types of experimental time dependencies: (1) the dependence of gas volume $q(t)$ or (2) the dependences of gas flow rate $J(t)$, permeated through a membrane. The pulse function variation of gas concentration in upstream is applied enough rare in experimental studies and corresponding response function $j(t)$ in downstream relates with other functions as follows:

$$j(t) = \frac{dJ(t)}{dt} = \frac{d^2 q(t)}{dt^2} \tag{8}$$

The unsteady selectivity for a gas pair can be expressed using Eq. (7) as follows:

$$\alpha_{US} = \frac{D^A S^A\left\{1+2\sum_{n=1}^{\infty}(-1)^n \exp\left(-\frac{n^2\pi^2 D^A t}{H^2}\right)\right\}}{D^B S^B\left\{1+2\sum_{n=1}^{\infty}(-1)^n \exp\left(-\frac{n^2\pi^2 D^B t}{H^2}\right)\right\}} \tag{9}$$

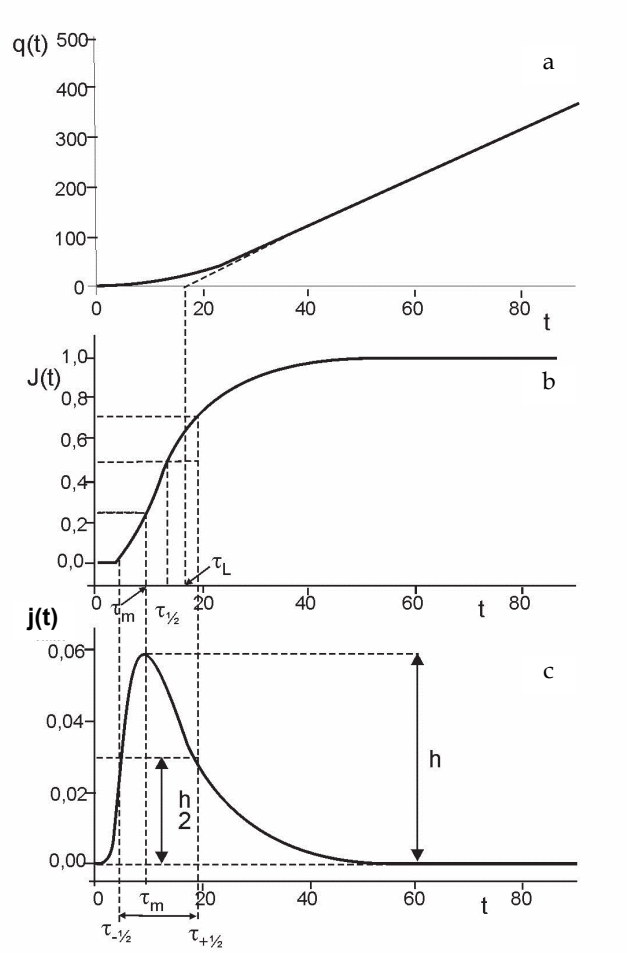

Fig. 1. Typical kinetic curves for different experimental methods of measurements of unsteady gas transfer: a – integral method (variation of gas volume in downstream after step function variation of gas concentration in upstream), b – differential method (variation of gas flux in downstream after step function variation of gas concentration in upstream), c – pulse method (variation of gas flux in downstream after pulse function variation of gas concentration in upstream).

As it is seen from eq. (9) the non steady-state selectivity factor (α_{US}) depends on diffusion time. Accordingly to Eq. (9) when $t \to \infty$, $\alpha_{US} \to \alpha_{SS}$ and the highest value of selectivity can be achieved at short times. The unsteady-state regime allows to rich infinitely high selectivity of separation but at the same time permeation fluxes dramatically go down. It means that for real application of unsteady separation regime the compromise time intervals need to be selected for appropriate balance between permeance and selectivity values.

2.2 Pulse function variation of gas concentration in upstream

In the case of pulse permeation method the measurement of the gas flux permeating through membrane as response on the short square pulse of feed concentration is considered (Beckman et al., 1989, 1991). In the case of the square pulse of concentration with duration Δt in upstream the response function of gas flux can be described as follows:

$$J(t) = J_{SS}\left[f_1(t) - \gamma f_2(t-\Delta t)\right], \tag{10}$$

where γ=0 for $t<\Delta t$ (the rising branch of curve) and γ=1 for $t>\Delta t$ (the descending branch of curve):

$$f_1(t) = 1 + 2\sum_{n=1}^{\infty}(-1)^n \exp\left(-n^2\pi^2 D\frac{t}{H^2}\right) \tag{11}$$

$$f_2(t) = 1 + 2\sum_{n=1}^{\infty}(-1)^n \exp\left(-n^2\pi^2 D\frac{t-\Delta t}{H^2}\right) \tag{12}$$

The distortion of pulse concentration at $\Delta t \to 0$ for the permeation through membrane is described by Eq. (13):

$$j(t) = \frac{dJ(t)}{dt} = 2J_{SS}\frac{\pi^2 D}{H^2}\sum_{n=1}^{\infty}(-1)^{n+1} n^2 \exp\left\{-\left(\frac{n\pi}{H}\right)^2 Dt\right\} \tag{13}$$

The permeation flux through the membrane is decreasing with decreasing of the pulse duration. As to compare with other permeability methods the pulse method requires shorter time of experiment and possesses higher resolution and dynamics.

The transfer of square pulse of concentration of binary gas mixture is considered below. If permeability coefficients of both components are similar (for example, hydrogen and carbon dioxide permeability as it can be found for main part of polymers) the separation of such gas mixture at steady-state condition is actually impossible. However, if values of diffusivity coefficients are not similar (for example $D_A > D_B$), the separation can be possible though at definite interval of time with very high selectivity factors. In this case the membrane acts as chromatography column. During this process at short times penetrate flux is enriched by component A, at average times both components are presented and at long times the component B is dominated in downstream. It should be noted that the resolution between two peaks is strongly depends on the pulse duration (Δt) and it decreases with increasing of Δt. Thus, the selectivity of separation can be controlled by the duration of pulse.

For the quantitatively description of the membrane separation process the differential unsteady selectivity factor can be introduced:

$$\alpha(t) = \frac{J_A(t)}{J_B(t)} = \frac{J_{SS\,A}F_A}{J_{SS\,B}F_B} = \alpha_{SS}K_\alpha, \tag{14}$$

where $F = J(t)/J_{SS}$, $\alpha_{SS} = S_A D_A/(S_B D_B)$ is the steady-state selectivity factor, $K_\alpha = F_A/F_B$ is the parameter of selectivity, and $\alpha(t)$ is the differential unsteady selectivity factor. It is evident that unsteady selectivity factor is transformed to the steady-state one if duration of the pulse increasing ($\Delta t \to \infty$, $K_\alpha \to 1$, $\alpha(t) \to \alpha_{SS}$). It should be noted that α_{SS} is determined by relation

of the permeability coefficients P_A and P_B, whereas K_α depends only on diffusivity coefficients. It allows controlling the penetrated gas mixture composition by variation of pulse duration and/or time of recovery.

It should be noted that in case of evident resolution of two concentration peaks after membrane the task of gas transfer parameters determination can be easily solved by using non-linear Least Squares Method (LSM): the diffusivity coefficients are determined by the time of peak's maximum achievement, and the solubility coefficients are estimated by heights of peaks.

In case of non-resolved peaks the following algorithm based on assumption of simple peak function can be suggested. First of all the time of maximal flux achievement (t_m) and maximal height of peak (I_m) have to be determined. Then the peak should be divided into n parts by height (for example n=10 and height of each part is h_i, Fig. 2). Each part has two characteristic points of intersection with curve $I(t)$: at time t_i^- and at time t_i^+, which determine width of peak at height h_i as $d_i = t_i^+ - t_i^-$ and two segments: left half-width $d_i^- = t_m - t_i^-$ and right half-width $d_i^+ = t_i^+ - t_m$. In such a way the ensemble of asymmetry parameters $\Delta_i = d_i^+ - d_i^-$ can be determined.

The advantage of suggested method is that it can be applied for the determination of diffusivity coefficients of gases for binary gas mixture of unknown composition. Such analysis can be important, for example, for applications where gas sensors with selective membrane layer are used. Particular nomographs for determination of gas diffusivities were calculated and are represented in Fig. 3. In this case the right half-widths of peak are used.

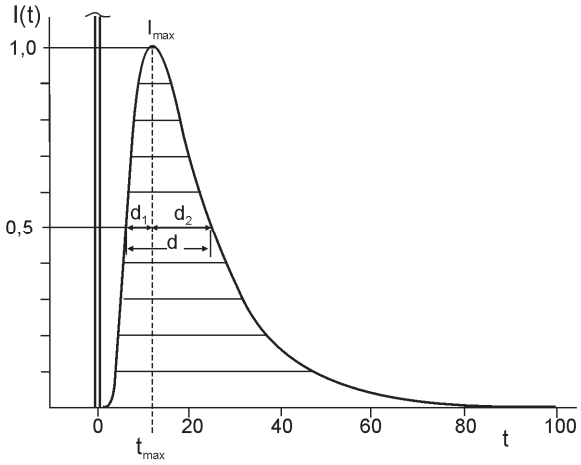

Fig. 2. The analysis of non-resolved peaks after membrane (infinitely short concentration pulse in upstream).

So, if to find these parameters from experimental peak and to fix the time of the peak maximum t_m, then to draw on diagram the experimental point, then to find the relation of the diffusion coefficients for binary gas mixture along with parallel, so, the relative contribution of D values can be found along with meridian. If to know the thermodynamic properties of gases considered and the diffusivity of main component the composition of the feed gas mixture and D value of second component can be determined.

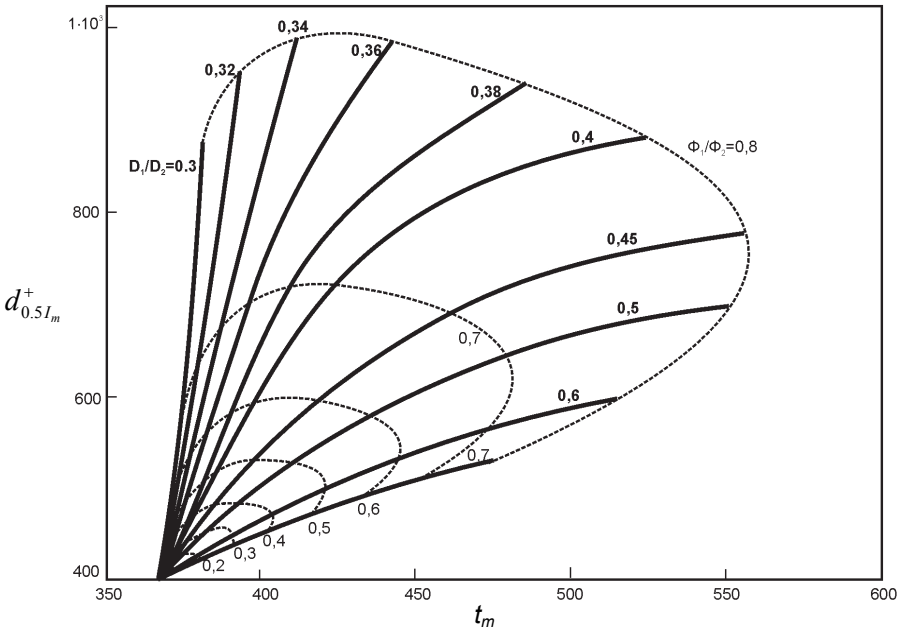

Fig. 3. Nomographs for the determination of the gas diffusivity coefficients and the composition of binary gas mixture. The parameters for the calculation are: H=0.02 cm, S_1/S_2=0.5, A_S=100 см², p=76 cm Hg. Φ_1 and Φ_2 are corresponding contributions into permeation flux of components A and B.

2.3 Harmonic function variation of gas concentration in upstream

Method of the concentration wave is based on study of wave deformation during penetration through a membrane. The variation of gas flux at the downstream is usually measured. Measurements should be carried out at several frequencies of harmonic function. Obtained dependencies of amplitude and phase variation on frequency are used for the characterization of membrane. The existing of five degrees of freedom (steady-state condition relatively of which the harmonic function takes place; time of the steady-state achieving; change of the amplitude and phase characteristics after transfer through membrane and their dependences on the frequency) allows to control the diffusion of gas and consequently the separation process (Beckman et al., 1996).

In case of variation of gas concentration in upstream as harmonic function:

$$C = 0.5C_0\left[1+\sin(\omega t)\right], \tag{15}$$

the variation of gas flux after membrane can be described by the following equation:

$$J_1 = \frac{DAC_0}{2H}\left\{\sin(\omega t) + 2\omega\sum_{n=1}^{\infty}\frac{(-1)^n\left\{\frac{n^2\pi^2 D}{H^2}\left[\cos(\omega t)-\exp\left(-\frac{n^2\pi^2 Dt}{H^2}\right)\right]+\omega\sin(\omega t)\right\}}{\frac{n^4\pi^4 D^2}{H^4}+\omega^2}\right\} \tag{16}$$

where $C_0 = Sp_0$, p_0 is maximal partial pressure of gas, ω is frequency.
Harmonic variation of gas flux after membrane will have the same frequency but lower amplitude and phase shift (Fig. 4).
If concentration of gas in upstream fluctuate with amplitude A_0:

$$C(0,t) = A_0 \sin(\omega t), \tag{17}$$

harmonic vibrations take place around stable level that can be calculated as follows:

$$J_R = \frac{A_0}{2}\left\{1 + 2\sum_{n=1}^{\infty}(-1)^n \exp\left(-\frac{n^2\pi^2 Dt}{H^2}\right)\right\} \tag{18}$$

At high values of time a quasi-stationary flux through membrane can be described as follows:

$$J(t) = \frac{DAC_0}{H}\left(\sin(\omega t) + 2\omega\sum_{n=1}^{\infty}\frac{(-1)^n\left\{\frac{n^2\pi^2 D}{H^2}\cos(\omega t) + \omega\sin(\omega t)\right\}}{\frac{n^4\pi^4 D^2}{H^4} + \omega^2}\right) \tag{19}$$

Eq. (19) represents the simple harmonic vibration that has the same frequency but lower amplitude and phase shift:

$$J_\infty(\omega) = A(\omega)\sin\left[\omega t + \varphi(\omega)\right], \tag{20}$$

where the amplitude of passed wave is:

$$A(\omega) = \frac{A_0 H\sqrt{\frac{\omega}{D}}}{\left[\mathrm{sh}^2\left(H\sqrt{\frac{\omega}{2D}}\right) + \sin^2\left(H\sqrt{\frac{\omega}{2D}}\right)\right]^{1/2}} \tag{21}$$

and the phase shift is:

$$\varphi(\omega) = \mathrm{arctg}\left[\frac{\mathrm{tg}\left(H\sqrt{\frac{\omega}{2D}}\right) - \mathrm{th}\left(H\sqrt{\frac{\omega}{2D}}\right)}{\mathrm{tg}\left(H\sqrt{\frac{\omega}{2D}}\right) + \mathrm{th}\left(H\sqrt{\frac{\omega}{2D}}\right)}\right] \tag{22}$$

Concentration waves decay strongly as a rule, however they possess all properties of waves, in particularly, interference and diffraction.
The diagram shown in Fig. 5 allows carrying out relatively simple estimation of diffusivity coefficient by measuring the ratio between the amplitude and the phase shift of the incident and the transmitted waves at definite frequency: the crossing point of the respective curves can be used for determination of D values. For small values of frequency following

simplified equation can be used: $\varphi=\omega H^2/6D$. For high values of frequency ($H\sqrt{\omega/2D} > \pi/2$) phase shift can be calculated as $\varphi \approx H\sqrt{\omega/2D} - \pi/4$.

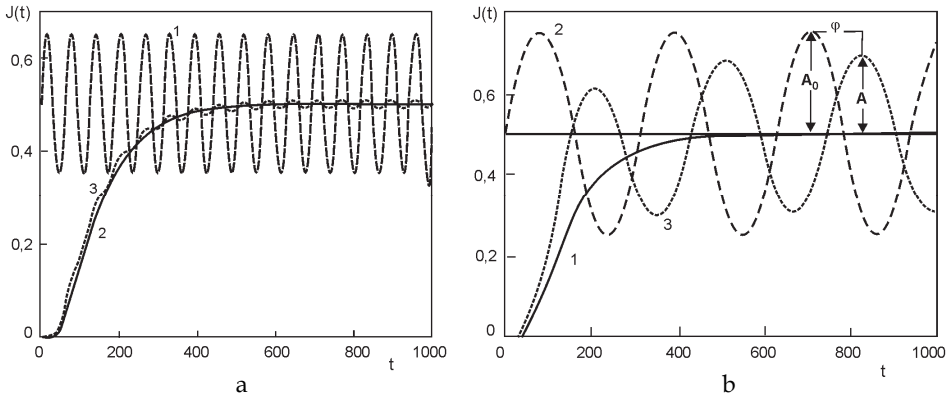

Fig. 4. The permeation of concentration wave through membrane (H=0.01 cm; D=10^{-7} cm^2/s) at two frequencies: $\omega = 0.1$ (a) and $\omega = 0.02$ (b). 1 – kinetic permeability curve (step function variation of the gas concentration in upstream); 2 – variation of the gas concentration in upstream; 3 – variation of the gas flux in downstream.

Thus, quasi-stationary gas flux value is determined by membrane permeance; the amplitude of the transmitted wave depends on permeability (i.e., on diffusivity and solubility coefficients), thickness of membrane and frequency. However, the ratio between the amplitude of the oscillations in upstream and downstream does not depend on the permeability coefficient. The phase shift depends on the diffusivity coefficient which determines the rate of the periodical stationary state achievement as well.

From experimental data treatment point of view this method possesses more degrees of freedom: time of the periodical stationary condition, the equilibrium position, the amplitude of wave and the phase shift. Diffusivity coefficient can be calculated by using of any of these parameters. Additional degree of freedom is changing of frequency.

For the classical diffusion mechanism the amplitude function $A(\omega)$ decreases with increasing of the frequency of waves (membrane passes the lower frequency waves and cut off the higher frequency ones); the phase shift function $\varphi(\omega)$ passes through minimum and then becomes as the periodical wave.

The particularity of permeation of the concentration waves through membrane is suitable to present as amplitude-phase diagram where the amplitude value represents the length of vector and the phase shift is the angle of slope. The swing of spiral is defined by the permeability coefficient P. If the amplitude-phase diagram to imagine as reduced value A/A_0, where A is the amplitude of transmitted wave and A_0 is the amplitude of the incident one then obtained curve will not depend on P and represents unique form for all variety of the situations of "classical" mechanism of diffusion.

It is evident that the membrane can be considered as the filter of high frequencies the higher diffusivity providing the wider the transmission band.

The permeation of concentration waves through non-homogeneous membrane media can be considered as a particular case. The example of gas diffusion by two parallel independent

channels (two-component medium) is considered below (corresponding parameters are: diffusivity coefficients D_1, D_2; solubility coefficients S_1, S_2; contributions to total flux through membrane $\Phi_1=S_1/S$, $\Phi_2=S_2/S$, where $S_1+S_2=S$, $\Phi_1+\Phi_2=1$.
The results of modeling are presented in Fig.6. It is seen that the presence of two ways of diffusion considerably changes the curve form of amplitude-phase characteristic. It can be used for the detection of additional channels of diffusion (e.g., pores) and for determination of values of local transport parameters.

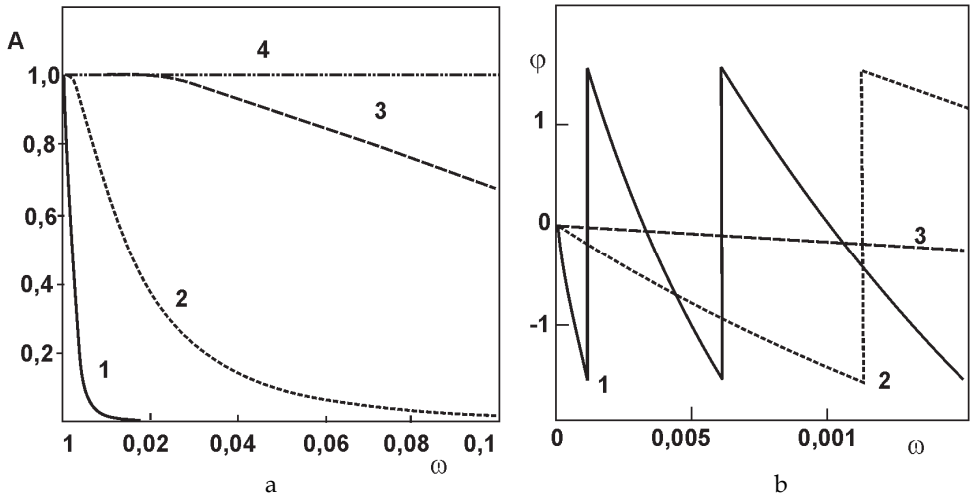

Fig. 5. The dependences of the amplitude and the phase shift of the transmitted wave on the frequency of the incident wave at the different diffusivity values (cm^2/s): 1 – 10^{-8}, 2 – 10^{-7}, 3 – 10^{-6}, 4 – 10^{-5}; (a) relative amplitude (A_d / A_0), (b) phase shift.

Other representation of results of the concentration wave method is the Lissajous figures. These figures are built in coordinates: the ordinate is the amplitude of transmitted concentration wave; the abscissa is the amplitude of incident wave (Fig. 7). In case of homogeneous diffusion medium (classical mechanism of diffusion) the Lissajous figure has the appearance of straight line passing through origin of coordinates and angular with 45° in relation to the abscissa axis. Lissajous figure does not depend on the vibration frequency for classical diffusion mechanism.
If concentration wave consists of two gases A and B the input of membrane is as following:

$$c^A = \frac{C_0^A}{2}\left[1+\sin(\omega t)\right] \text{ and } c^B = \frac{C_0^B}{2}\left[1+\sin(\omega t)\right] \tag{23}$$

The flux at the output of membrane:

$$J = J^A + J^B \tag{24}$$

The periodic stationary condition is achieved after some intermediate time the amplitude being:

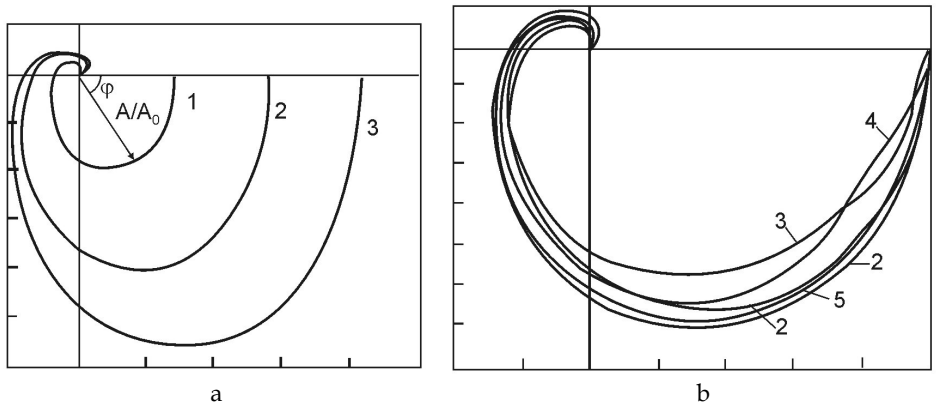

Fig. 6. The amplitude-phase diagrams obtained by the method of the concentration waves: a – (initial scale) homogeneous medium: 1 – D_1=l·10^{-5} cm^2/s, 2 – D_2=2·10^{-6} cm^2/s, 3 – parallel diffusion with D_1 and D_2 (Φ_1=Φ_2=0,5); b – reduced scale: 1 – homogeneous medium with any D, parallel diffusion with D_1= l·10^{-5} cm^2/s and D_2 (cm^2/s): 2 – 2·10^{-5}, 3 – 5·10^{-5}, 4 – 1·10^{-4}, 5 – 5·10^{-4}.

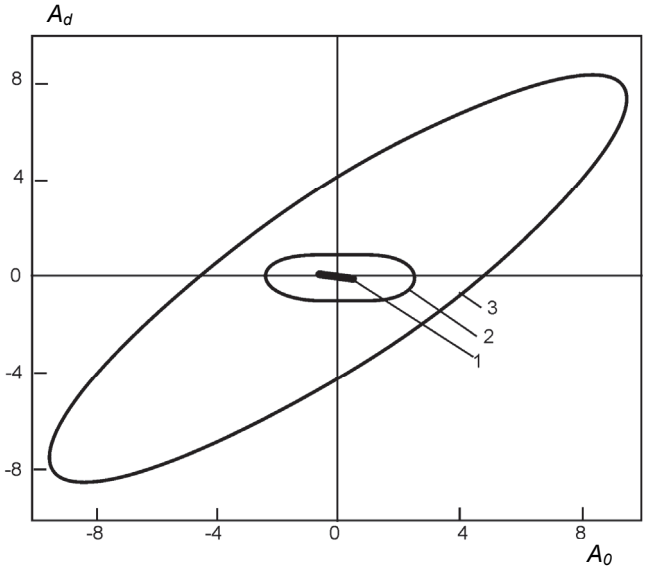

Fig. 7. Lissajous figure for the parallel diffusion through bicomponent membrane medium (D_1 = 1·10^{-5}, D_2 = 2·10^{-5} cm^2/s; Φ_1 = Φ_2 = 0.5): 1 – ω = 0.1 s^{-1}; 2 – ω = 0.5 s^{-1}; 3 – ω = 1 s^{-1}.

$$A = A^A \sin\left(\omega t + \varphi^A\right) + A^B \sin\left(\omega t + \varphi^B\right) = A^{AB} \sin\left(\omega t + \varphi^{AB}\right), \quad (25)$$

where $A^{AB} = \sqrt{\left(A^A\right)^2 + \left(A^B\right)^2 + 2A^A A^B \cos\left(\varphi^B - \varphi^A\right)}$ and the phase shift is:

$$\varphi^{AB} = \operatorname{arctg}\left(\frac{\varphi^B \sin\left(\varphi^B - \varphi^A\right)}{A^A + A^B \cos\left(\varphi^B - \varphi^A\right)}\right), \quad (26)$$

It should be noted that for lower frequency the amplitude of wave at output of membrane is defined by the both gas components. With increasing of the frequency the relative amplitude passes through minimum. This minimum on the curve $A^{AB}(\omega)/A^A$ via ω is defined by fact that the phase shift between output waves of components $\varphi^{AB} = |\varphi^A - \varphi^B| \rightarrow \pi/2$ leads to decreasing of total value of the amplitude at output of membrane. For enough high frequency ω, the amplitude A^B of the frequency with lower D value is small and total amplitude of output waves A is mainly defined by the amplitude of the component possessing high D value.

3. Separation of gas mixtures

Let's consider the separation of ternary gas mixtures at the different non-steady state regimes of permeation. The gas mixture will consist of oxygen, nitrogen and xenon (gaseous mixture of this kind is used in medicine). Traditionally, we have deal with the step function variation of gas concentration on input surface of membrane while the concentration is keeping to zero at output surface of membrane during whole duration of experiment. The calculation was carried out for the following parameters: H=0.01 cm, A=10 cm^2, p=1 bar, t=1 – 8000 sec, the diffusivity coefficients D are: $7.6 \cdot 10^{-7}$ (O_2), $3.6 \cdot 10^{-7}$ (N_2), $2.7 \cdot 10^{-8}$ (Xe); the solubility coefficients S are: $5.79 \cdot 10^{-3}$ (O_2), $3.06 \cdot 10^{-3}$ (N_2), $6.3 \cdot 10^{-2}$ (Xe); the permeability coefficients P are: $4.4 \cdot 10^{-9}$ (O_2), $1.102 \cdot 10^{-9}$ (N_2), $1.795 \cdot 10^{-9}$ (Xe), the steady state fluxes at output of membrane are: $3.344 \cdot 10^{-4}$(O_2), $8.372 \cdot 10^{-5}$(N_2), $1.293 \cdot 10^{-4}$ (Xe).

The steady state selectivity for the above mentioned gases are $\alpha_{O2/N2}$=4, $\alpha_{Xe/N2}$=1.54, $\alpha_{O2/Xe}$=2.59. From kinetic curves presented in Fig. 8(a) it is seen that the steady state condition is earlier achieved for oxygen and later on for xenon. It should be noted that the flux of nitrogen lower than one for xenon. The variation of the selectivity factors with time is shown in Fig. 8(b). For short-delay the selectivity can rich very high values but fluxes are very small. With time the non-stationary selectivity are tended to the stationary ones.

The calculation for the pulse function variation of gas concentration was carried out for ternary gas mixture oxygen-nitrogen-xenon (Fig.9). Xenon passes through membrane substantially later then oxygen and nitrogen though the steady state flux of xenon is higher than one for nitrogen. The steady state fluxes are 79.2 (oxygen), 19.8 (nitrogen) and 30.6 (xenon).

It should be noted that for the pulse variation of concentration the earlier fractions of oxygen and nitrogen are depleted by xenon but the final fractions involve a small content of oxygen and xenon being more than nitrogen. It is important that during permeation process the inversion of the selectivity occurs for pair nitrogen/xenon. For example, at time t = 1000 s

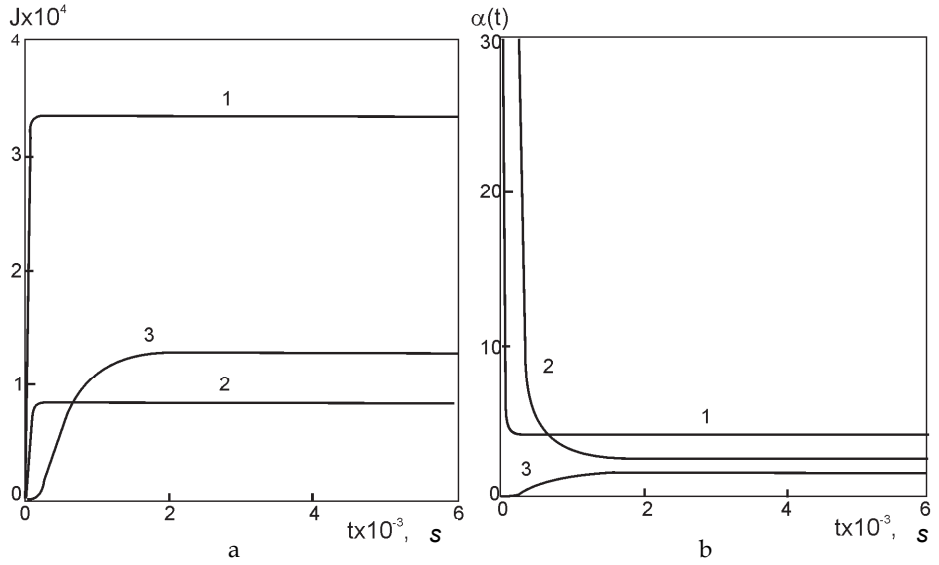

Fig. 8. Non-steady state permeability of oxygen (1), nitrogen (2) and xenon (3) through film of PVTMS: a – changing of gas fluxes with time at output of membrane; b – changing of separation selectivity with time: 1 – O_2/N_2, 2 – O_2/Xe, 3 – Xe/N_2.

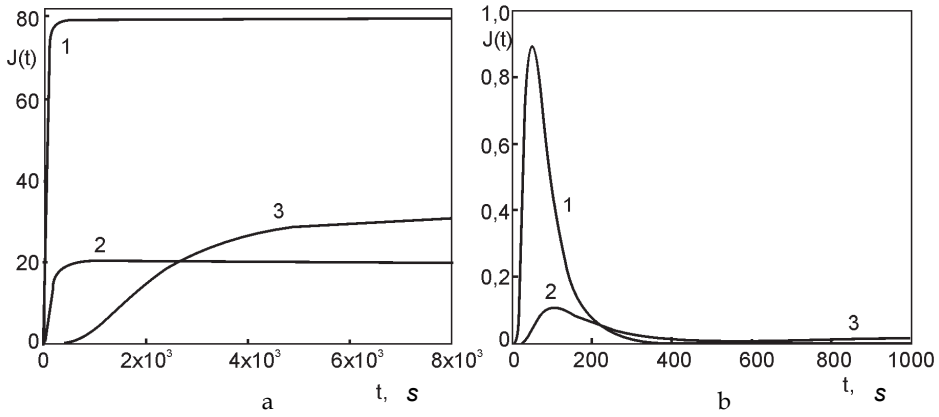

Fig. 9. Non-steady state permeability of oxygen (1), nitrogen (2) and xenon (3) through the film of PVTMS: a – the step variation of concentration; b – the pulse variation of concentration.

$\alpha(t) = J_{N_2} / J_{Xe}$ = 6.05, and at $t \to \infty$ α=0.65. It is evident that at time 2500-3000 s the separation of nitrogen/xenon mixture does not occur (α=1). In the whole, for the pulse variation of concentration xenon is well separated from air that we can clearly see in Fig. 10 where peaks are well resolved.

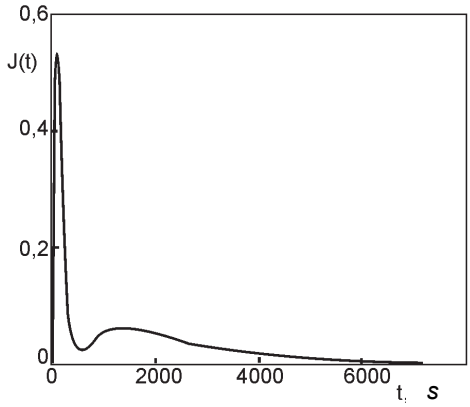

Fig. 10. The view of the output pulse function of gas mixture (nitrogen-xenon) permeation through PVTMS film.

The separation of considered ternary gas mixture is possible under the concentration wave regime as well. The results of mathematical modeling of permeation of the concentration wave (of nitrogen, oxygen or xenon) were obtained for PVTMS film. Following values of parameters were used for calculations: thickness of film H=0.01 cm; area A=10 cm^2; reference frequency: ω_0= 0.01 s^{-1} (range of frequency 0-0.04 s^{-1}); time interval: t=0-4000 s; feed pressure p_u=76 cm Hg; amplitude of the pressure variation in upstream is 15.2 cm Hg. (i.e., the feed pressure is 1 bar and harmonic changing is Δp=20%); transport parameters for oxygen: S=5.79·10^{-3} cm^3(STP)/(cm^3·cmHg), D=7.6·10^{-7} cm^2/s, P=4.4·10^{-9} cm^3(STP)·cm/(cm^3·s·cmHg); transport parameters for nitrogen: S=3.06·10^{-3} cm^3(STP)/(cm^3·cmHg), D=3.6·10^{-7} cm^2/s, P=1.1·10^{-9} cm^3(STP)·cm/(cm^3·s·cmHg). The flux is presented as cm^3(STP)/(s·cmHg) for all cases.

If to consider the separation of binary mixtures xenon-oxygen and xenon-nitrogen that the calculations were carried out using the same parameters as the above mentioned but the reference frequency was chosen lower: ω=0.001, the range of frequency was 0-0.003 s^{-1}, time range t=0-10000 s, D_{Xe} 2.7·10^{-8}, S_{Xe}=0.63, P_{Xe}=1.7·10^{-9}. The stationary selectivity for oxygen/xenon α=2.59. Since for PVTMS we have P_{O2}>P_{Xe}>P_{N2}, the maximal flux is for oxygen (3.34·10^{-3}), then for xenon (8.37·10^{-5}) and then for nitrogen (1.28·10^{-4}). The oscillations of output waves of gas fluxes with amplitudes 6.69·10^{-5}, 1.67·10^{-5}, 2.41·10^{-5} and with the phase shift 0.022, 0.046 and 0.685 for oxygen, xenon and nitrogen, respectively (since D_{O2}>D_{N2}>D_{Xe}).

Fig. 11 demonstrates the particularity of the flux fluctuations for mixtures xenon-oxygen as transmitted waves for PVTMS film. It was found that the fluxes relatively of which the harmonic vibration occurs are varied from 1.623·10^{-4} for mixture with 10% Xe till 3.166·10^{-4} for mixture with 90%Xe; the wave amplitude from 2.593·10^{-5} for mixture with 10% Xe till 6.154·10^{-5} for mixture with 90%Xe, the phase shift from 0.505 for mixture with 10% Xe till 0.043 for mixture with 90%Xe. In the range of given interval of frequency the wave amplitudes of oxygen and nitrogen do not practically depend on the frequency whereas the xenon amplitude decreases. The selectivity factor fluctuates on periodical (but not sinusoidal) low: the fluctuations are substantial for gas mixtures enriched by Xe and lower for ones with lower content of Xe.

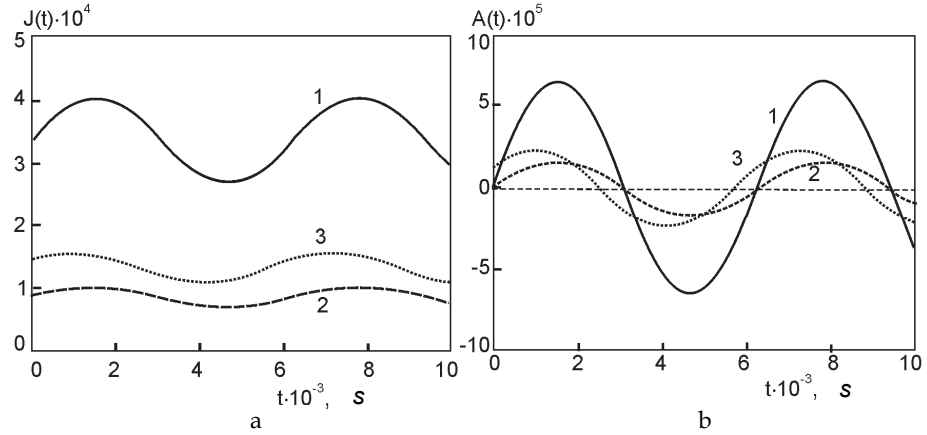

Fig. 11. The concentration waves at the output of membrane for mixture oxygen (30%), xenon (30%) and nitrogen (40%): a – flux fluctuation, b – the variation of the oscillation swing for different gases: 1 – oxygen, 2 – nitrogen, 3 – xenon.

4. Control of gas transfer in membranes

Previously there were considered methods of influence on membrane separation characteristics by variation of conditions at the upstream membrane side. Another group of methods is based on the modification of a membrane i.e. introduction of functional groups into membrane material that leads to acceleration or slowing down of diffusion of one of gas mixture components. Demonstration of application of these methods is presented below.

4.1 Acceleration of diffusion of a component

The improvement of separation can be achieved under as steady as unsteady state conditions by introduction of additional diffusion channel for one of gas mixture components. The model of dissociation diffusion can be applied for this case. The model considers two diffusion channels with diffusion coefficients D_1 and D_2 for a component transfer and possibility of molecules exchange between channels with transition rate constants k_1 and k_2 for transition from channel 1 to 2 and vice versa respectively (equilibrium constant of transition $K = k_1/k_2$). In this case differential equation system of component transfer is as follows:

$$\begin{cases} \dfrac{\partial C_1}{\partial t} = D_1 \dfrac{\partial^2 C_1}{\partial x^2} - k_1 C_1 + k_2 C_2 \\ \dfrac{\partial C_2}{\partial t} = D_2 \dfrac{\partial^2 C_2}{\partial x^2} + k_1 C_1 - k_2 C_2 \end{cases}, \tag{27}$$

where C_1 and C_2 – gas concentration in channels 1 and 2, D_1 and D_2 – diffusion coefficients of gas in channels 1 and 2, k_1 – probability of transition 1→2, k_2 – probability of transition 2→1.
The solution of the system for flat thin film with thickness H and traditional boundary conditions is:

1. Gas flow rate in channel 1:

$$J_1(t) = J_{SS1}\left[1 - \sum_{n=1}^{\infty} \frac{(-1)^n}{A}\left\{\left(\alpha_1 - D_2\omega_n^2 - k_1 - k_2\right)e^{-\alpha_1 t} - \left(\alpha_2 - D_2\omega_n^2 - k_1 - k_2\right)e^{-\alpha_2 t}\right\}\right] \quad (28)$$

2. Gas flow rate in channel 2:

$$J_2(t) = J_{SS2}\left[1 - \sum_{n=1}^{\infty} \frac{(-1)^n}{A}\left\{\left(\alpha_1 - D_1\omega_n^2 - k_1 - k_2\right)e^{-\alpha_1 t} - \left(\alpha_2 - D_1\omega_n^2 - k_1 - k_2\right)e^{-\alpha_2 t}\right\}\right] \quad (29)$$

where $\omega = \pi n / H$,

$$J_{SS1} = \frac{AD_1S_1p_u}{H} \quad (30)$$

$$J_{SS2} = \frac{AD_2S_2p_u}{H} \quad (31)$$

$$\alpha_1(\omega) = 0.5\left[\left(D_1 + D_2\right)\omega^2 + k_1 + k_2\right] - A(\omega) \quad (32)$$

$$\alpha_2(\omega) = \alpha_1(\omega) + 2A(\omega) \quad (33)$$

$$A(\omega) = 0.5\sqrt{\left(D_1 - D_2\right)^2\omega_n^4 + 2\left(D_1 - D_2\right)\left(k_1 - k_2\right)\omega_n^2 + \left(k_1 + k_2\right)^2}\ , \quad (34)$$

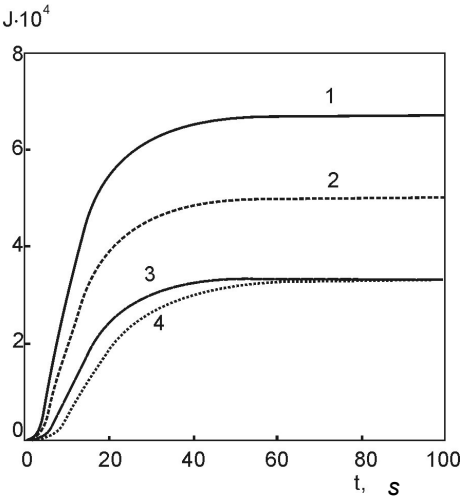

Fig. 12. Unsteady oxygen flow rate through PVTMS membrane: 1 – oxygen flow rate in channel 1, 2 – overall flow rate (individual flow rates are involved with weight 0.5), 3 – oxygen flow rate in channel 2, 4 – oxygen flow rate for classical diffusion mechanism.

Overall flow rate through membrane (with contribution of each flux 0.5) is:

$$J(t) = 0.5\left[J_1(t) + J_2(t)\right] \tag{35}$$

Calculation was carried out with following values of parameters: A=10, H=0.01, p=76, t=1-200. It was assumed that dissociation diffusion mechanism is realized for oxygen while transfer of nitrogen occurs by classical diffusion mechanism. Parameters for oxygen: D_1=7.6x10^{-7}, D_2=D_1, S_2=S_1=5.79x10^{-3}, k_1=0.1 and k_2=0.1 (K=1). Parameters for nitrogen: D=3.6x10^{-7}, S=3.06x10^{-3}. Obtained dependencies are presented in Fig. 12. One can see that additional channel decreases the time of unsteady state.

Fig. 13 represents unsteady separation factor for oxygen/nitrogen gas pair. Introduction of additional diffusion channel increases value of separation factor α (steady state value increases from 4 to 6). Transition rate constants have no influence on steady state separation factor value. At initial time increasing of K leads to increasing of separation factor but these effects are relatively small.

The influence of introduction of additional diffusion channel on separation when pulse function variation of gas concentration in upstream is applied is shown in Fig. 14. Calculation was carried out for the same parameters determined above except D_2=5D_1. Oxygen transfer by dissociation diffusion mechanism (diffusion in two parallel channels with reversible exchange of gas molecules among them) leads to drastic increase of peak height and its displacement to lower times compared to classical diffusion mechanism.

Fig. 15 represents similar data for air (21% of O_2, 78% of N_2). In case of diffusion by classical mechanism there is no clear separation while in case of dissociation diffusion of oxygen (and classical diffusion of nitrogen) at k_1=k_2=0.1 (K=1) the bimodal shape of overall peak is noticeable due to displacement of oxygen peak to lower times. When transition rate constants are k_1=1 and k_2=0,1 (K=10) overall peak clearly expands to two components so that almost pure oxygen passes through membrane at lower times and nitrogen at higher times.

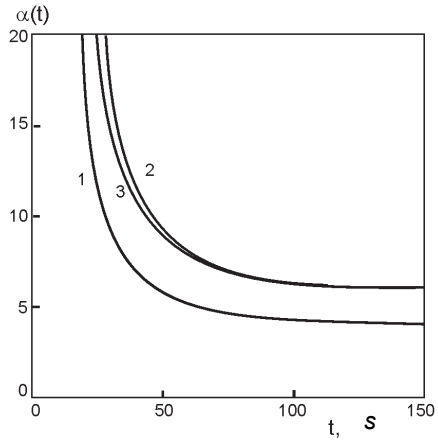

Fig. 13. Unsteady separation factor $\alpha_{O2/N2}$: 1 – "classical" diffusion, 2 – K=1, 3 – K=10.

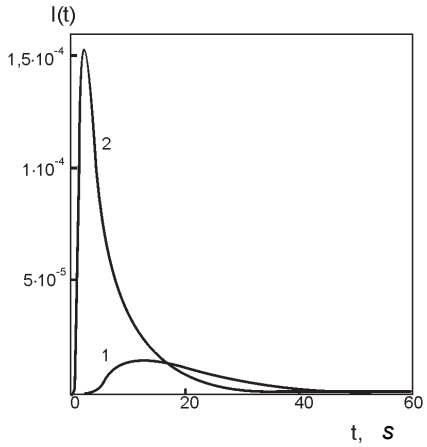

Fig. 14. Comparison of oxygen concentration peaks deformation for delta-function impulse transfer through PVTMS membrane: 1 – oxygen diffusion by classical mechanism, 2 – oxygen diffusion by dissociation mechanism.

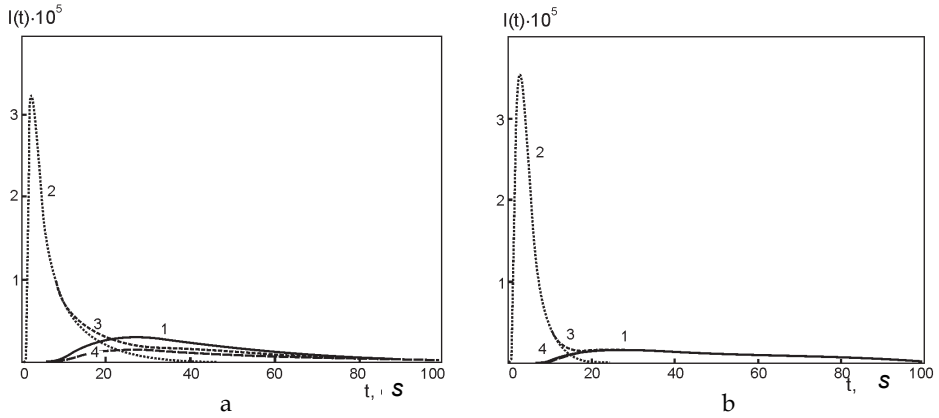

Fig. 15. Separation of air, pulse function variation of gas concentration in upstream: a – transition rate constants k_1=k_2=0.1 (K=1), b – transition rate constants k_1=1, k_2=0.1 (K=10). 1 – air transfer by classical diffusion mechanism; dissociation diffusion of oxygen: 2 – oxygen flow rate, 3 – overall flow rate, 4 – nitrogen flow rate.

4.2 Slowing down of diffusion of a component

Another approach of improvement of membrane separation characteristics under unsteady mass transfer conditions is slowing down of diffusion of one of gas mixture components. Such effect can be achieved by introduction of chemically active centers (functional groups) into membrane material which one of gas mixture components reacts with. In case of the first order reversible chemical reaction the mass transfer of reacting component is described by following differential equation system:

$$\begin{cases} \dfrac{\partial C_1}{\partial t} = D_1 \dfrac{\partial^2 C_1}{\partial x^2} - k_1 C_1 + k_2 C_2 \\ \dfrac{\partial C_2}{\partial t} = k_1 C_1 - k_2 C_2 \end{cases}, \tag{36}$$

where C_1 and C_2 – component concentration in membrane medium and chemically active centers, respectively, D – diffusion coefficient, k_1 and k_2 – primary and reversible chemical reaction rate constants, respectively.

System (36) has analytical solution. Unsteady gas flow rate trough membrane can be expressed as follows:

$$J = \frac{DSAp_u}{H}\left\{1 - \sum_{n=1}^{\infty} \frac{(-1)^n}{A}\left[\left(\alpha_1 - k_1 - k_2\right)e^{-\alpha_1 t} - \left(\alpha_2 - k_1 - k_2\right)e^{-\alpha_2 t}\right]\right\}, \tag{37}$$

where $\omega = n\pi/H$, n=1, 2, ...,

$$\alpha_1 = 0.5\left(k_1 + k_2 + D\omega^2\right) - A \tag{38}$$

$$\alpha_2 = 0.5\left(k_1 + k_2 + D\omega^2\right) + A \tag{39}$$

$$A = \sqrt{k_1 k_2 + 0.25\left(k_1 - k_2 + D\omega^2\right)^2} \tag{40}$$

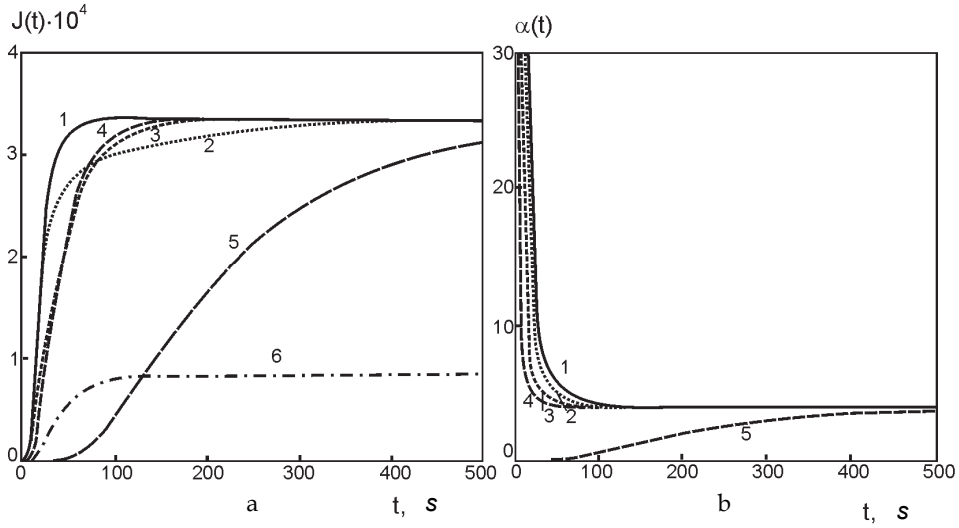

Fig. 16. The influence of reversible chemical sorption on unsteady oxygen transfer: a – unsteady oxygen flow rate; b – unsteady separation factor (1 – diffusion of oxygen by classical mechanism; diffusion with chemical sorption: 2 – k_1=k_2=0.01; 3 – k_1=k_2=0.1; 4 – k_1=k_2=1; 5 – k_1=10, k_2=1; 6 – unsteady nitrogen transfer).

Calculation was carried out with the same main parameters which were defined in previous section. Fig. 16(a) represents the influence of chemical sorption and values of reaction rate constants on unsteady oxygen flow rate through membrane, and Fig. 16(b) represents the influence of these parameters on unsteady oxygen/nitrogen separation factor. Figures demonstrate that capture of oxygen by chemically active centers significantly affect the shape of flow rate curves, especially at high values of chemical equilibrium constant ($K=k_1/k_2$). Capture of oxygen leads to slowing down of its diffusion and decreasing of efficiency of oxygen from nitrogen separation.

4.3 Example of modeling of unsteady CO2 transfer in liquid membrane with chemical absorbent

It is known that insertion of practically interesting quantities of immobilization centers into polymer matrix can be difficult. At the same time there is a class of membranes where insertion of desirable substances in membrane media is very simple. This class is represented by liquid membranes (LMs). In spite of their disadvantages such as degradation, complexity of preparation, sensitivity to pressure drop etc., LMs show extremely high selectivity for particular gas pares and are interesting as an object of fundamental studies. Practical example of theoretical description and calculation of unsteady CO_2 transfer in LM and the comparison of theoretical results with experimental data is presented in this section.

It was shown experimentally that step function supply of CO_2/N_2 gas mixture over LM with aqueous potassium carbonate (chemical absorbent of CO_2) results in establishing of the steady N_2 flux through the membrane after 50 seconds while CO_2 flux through the membrane rises only up to 10% of the steady state value after 250 seconds in spite of almost equal magnitudes of N_2 and CO_2 diffusion coefficients. Such slow increasing of CO_2 flow rate is caused by interaction of CO_2 with carbonate ions that leads to formation of bicarbonate ions. This situation is simultaneously similar to both ones described in previous sections: capture of CO_2 molecules on the one hand and its additional transfer due to diffusion and reversible reaction of bicarbonate ions with releasing of CO_2 on the other side of membrane on the other hand. Therefore the time of achievement of the steady state of CO_2 transfer is higher (due to CO_2 capture) and final value of CO_2 flow rate is also higher (due to additional CO_2 transfer in bicarbonate ion form) compared to the case where chemical absorption is absent. This example shows that under unsteady state conditions such membrane provides N_2-rich permeate at the beginning and CO_2-rich permeate after certain time (since steady-state CO_2 permeance is higher).

The description and analysis of CO_2 transfer in this case is more complex than described in previous sections because carbonate ions are mobile and can be considered as CO_2 "carriers" that introduces the necessity to take into account their transfer in LM as well as transfer of CO_2 in the form of bicarbonate ions and interactions between all reactants. Another particularity of considered example is that reaction of CO_2 with aqueous potassium carbonate is the second order reversible chemical reaction therefore analytical solution of differential equation system of mass transfer can not be obtained. Numerical methods of the differential equation system solution are the only that can be applied for calculations. The scheme and coordinates of considered LM is shown in Fig. 17. LM is formed between two polymeric membranes which are asymmetric with thin dense layer turned to the liquid phase. The permeance of polymeric membranes is two orders higher than permeance of LM and thickness of dense layer is three orders lower than thickness of LM. The time of establishing of steady state mass transfer through polymeric membranes is four orders

lower than for LM, therefore unsteady mass transfer in polymeric membranes can be neglected. Presented below mathematical model of CO_2 transfer in LM with aqueous potassium carbonate is based on the following assumptions: isothermal conditions; diffusion and solubility coefficients of the components are independent from concentration changes caused by diffusion and chemical reactions; components of gas phase (i.e. CO_2, N_2 etc.) are the only volatile species; a negligible change in the liquid phase volume during absorption of volatile components; concentration of volatile components in molecular form in the membrane and the liquid phase obeying Henry's law.

The approach of CO_2 interaction with aqueous potassium carbonate can be found in numerous studies (Cents et al., 2005; Chen et al., 1999; Danckwerts & Sharma, 1966; Dindore et al., 2005; Lee et al., 2001; Morales-Cabrera et al., 2005; Otto & Quinn, 1971; Pohorecki & Kucharski, 1991; Suchdeo & Schultz 1974; Ward & Robb, 1967).

The mechanism is based on accounting of four reactions. When potassium carbonate dissolves in water it dissociates with formation of metal and carbonate ions. The reaction of carbonate ions with water gave rise to bicarbonate and hydroxyl ions:

$$CO_3^{2-} + H_2O \overset{K_C'}{\Leftrightarrow} HCO_3^- + OH^- \tag{41}$$

Almost in all the studies mentioned above this reaction (and corresponding expression for calculation of the reaction equilibrium constant) is given in the following alternative form:

$$HCO_3^- + H_2O \overset{K_C}{\Leftrightarrow} H_3O^+ + CO_3^{2-} \tag{42}$$

These two reactions are interconnected by the reaction of dissociation of water:

$$2H_2O \overset{K_W}{\Leftrightarrow} H_3O^+ + OH^- \tag{43}$$

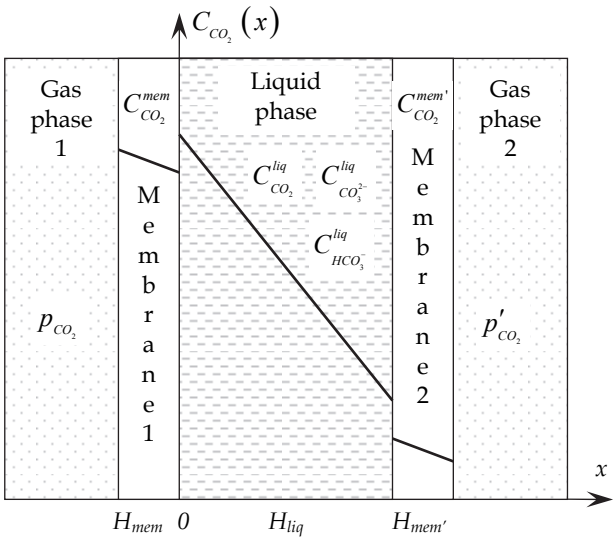

Fig. 17. The scheme and coordinates of LM used in mathematical model.

The interaction of CO_2 with the potassium carbonate solution occurs by two parallel reactions:

$$CO_2 + 2H_2O \underset{k_{-1}}{\overset{k_1}{\Leftrightarrow}} H_3O^+ + HCO_3^- \tag{44}$$

$$CO_2 + OH^- \underset{k_{-2}}{\overset{k_2}{\Leftrightarrow}} HCO_3^- \tag{45}$$

The overall reaction of CO_2 with carbonate ion can be represented as follows:

$$CO_2 + CO_3^{2-} + H_2O \Leftrightarrow 2HCO_3^- \tag{46}$$

Reactions (44) and (45) are rate controlling reactions and reactions (41) and (43) can be considered as instantaneous reactions. Therefore concentrations of H_3O^+, OH^- and CO_3^{2-} are assumed to be always in equilibrium that allows to define reaction rate term of CO_2 as follows:

$$R_{CO_2}^{liq} = C_{HCO_3^-}^{liq}\left(k_{-1}K_C\frac{C_{HCO_3^-}^{liq}}{C_{CO_3^{2-}}^{liq}} + k_{-2}\right) - C_{CO_2}^{liq}\left(k_1 + k_2\frac{K_W C_{CO_3^{2-}}^{liq}}{K_C C_{HCO_3^-}^{liq}}\right) \tag{47}$$

Reaction rate terms of CO_3^{2-} and HCO_3^- are following from Eq. (46):

$$R_{CO_3^{2-}}^{liq} = R_{CO_2}^{liq} \tag{48}$$

$$R_{HCO_3^-}^{liq} = -2R_{CO_2}^{liq} \tag{49}$$

Here it is assumed that the activity coefficients of all species are equal to unity. Equations permitting calculations of the reaction rate and equilibrium constants can be found in the literature and are presented in Table 1.

Thus, in addition to the CO_2 transfer in the liquid phase it is necessary to take into account the transfer and interaction of carbonate ions and bicarbonate ions. The differential equation system of unsteady mass transfer in liquid phase can be represented as follows:

$$\begin{cases} \dfrac{\partial C_{CO_2}^{liq}(x,t)}{\partial t} = D_{CO_2}^{liq}\dfrac{\partial^2 C_{CO_2}^{liq}(x,t)}{\partial x^2} + R_{CO_2}^{liq}(x,t) \\ \dfrac{\partial C_{CO_3^{2-}}^{liq}(x,t)}{\partial t} = D_{CO_3^{2-}}^{liq}\dfrac{\partial^2 C_{CO_3^{2-}}^{liq}(x,t)}{\partial x^2} + R_{CO_2}^{liq}(x,t) \\ \dfrac{\partial C_{HCO_3^-}^{liq}(x,t)}{\partial t} = D_{HCO_3^-}^{liq}\dfrac{\partial^2 C_{HCO_3^-}^{liq}(x,t)}{\partial x^2} - 2R_{CO_2}^{liq}(x,t) \end{cases} \tag{50}$$

Boundary conditions at the membrane-gas phase interface:

$$C_{CO_2}^{m}(-H_m,t) = p_{CO_2}(t)S_{CO_2}^{m} \tag{51}$$

Constant	Equation	Units	Ref.
k_1	$\log_{10} k_1 = 329.85 - 110.541 \log_{10} T - 17265.4 / T$	s^{-1}	Danckwerts & Sharma, 1966
k_2	$\log_{10} k_2 / k_2^{\infty} = 0.08I$	l/(mol·s)	Rahimpour & Kashkooli, 2004
	$\log_{10} k_2^{\infty} = 13.635 - 2895 / T$	l/(mol·s)	Danckwerts & Sharma, 1966
K_1	$\log_{10} K_1 = 14.843 - 0.03279T - 3404.7 / T$	mol/l	Danckwerts & Sharma, 1966
K_2	$K_2 = K_1 / K_4$	l/mol	Danckwerts & Sharma, 1966
K_C	$\log_{10} K_C^{\infty} = 6.498 - 0.0238T - 2902.4 / T$	mol/l	Danckwerts & Sharma, 1966
K_W	$\log_{10} K_W = -23.5325 + 0.03184T$	mol^2/l^2	Lee et al., 2001
D_{CO_2}	$D_{CO_2} = \frac{0.0235 \times \exp(-2119 / T)}{(1 + 0.354M)^{0.82}}$	cm^2/s	Lee et al., 2001
$D_{HCO_3^-}$	$D_{HCO_3^-} = D_{CO_3^{2-}} = D_{CO_2} \sqrt{\mu_{CO_2} / \mu_{HCO_3^-}}$	cm^2/s	Otto & Quinn, 1971
S_{CO_2}	$\log_{10} S_{CO_2} = -5.30 + 1140 / T - 0.125M$	mol/(l·atm)	Lee et al., 2001

Table 1. Values employed in the calculations.

$$C_{CO_2}^{m'}(H_{liq} + H_{m'}, t) = p'_{CO_2}(t) S_{CO_2}^{m'} \tag{52}$$

Boundary conditions at the membrane-liquid phase interface:

$$\frac{C_{CO_2}^{liq}(0,t)}{S_{CO_2}^{liq}} = \frac{C_{CO_2}^{m}(0,t)}{S_{CO_2}^{m}} \tag{53}$$

$$\frac{C_{CO_2}^{m'}(H_{liq},t)}{S_{CO_2}^{m'}} = \frac{C_{CO_2}^{liq}(H_{liq},t)}{S_{CO_2}^{liq}} \tag{54}$$

$$D_{CO_2}^{liq} \frac{\partial C_{CO_2}^{liq}(0,t)}{\partial x} = D_{CO_2}^{m} \frac{C_{CO_2}^{m}(0,t) - C_{CO_2}^{m}(-H_m,t)}{H_m} \tag{55}$$

$$D_{CO_2}^{liq} \frac{\partial C_{CO_2}^{liq}(H_{liq},t)}{\partial x} = D_{CO_2}^{m'} \frac{C_{CO_2}^{m'}(H_{liq} + H_{m'},t) - C_{CO_2}^{m'}(H_{liq},t)}{H_{m'}} \tag{56}$$

$$\frac{\partial C_{CO_3^{2-}}^{liq}(0,t)}{\partial x} = \frac{\partial C_{CO_3^{2-}}^{liq}(H_{liq},t)}{\partial x} = \frac{\partial C_{HCO_3^-}^{liq}(0,t)}{\partial x} = \frac{\partial C_{HCO_3^-}^{liq}(H_{liq},t)}{\partial x} = 0 \tag{57}$$

Initial conditions:

$$C^{liq}_{CO_2}(x,0) = \overline{C}^{liq}_{CO_2} \tag{58}$$

$$C^{liq}_{CO_3^{2-}}(x,0) = \overline{C}^{liq}_{CO_3^{2-}} \tag{59}$$

$$C^{liq}_{HCO_3^{-}}(x,0) = \overline{C}^{liq}_{HCO_3^{-}} \tag{60}$$

This model can be extended for the description of gas mixture transfer by addition of mass transfer equations of other components. The comparison between calculation and experimental data is shown in Figs. 18 and 19.

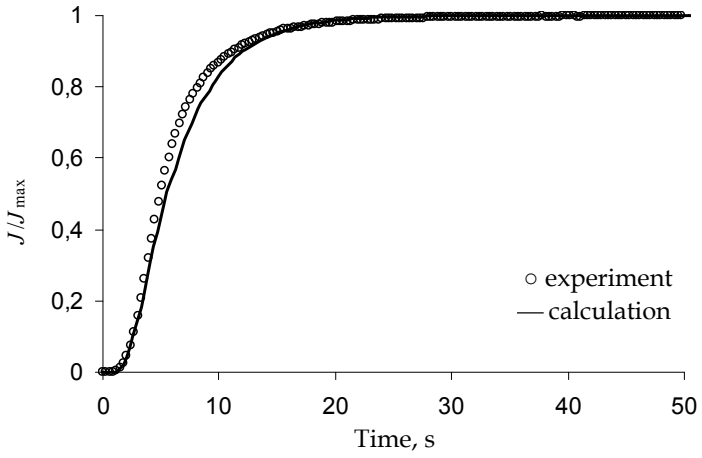

Fig. 18. Unsteady CO_2 transfer through LM with distilled water.

Theoretical and experimental dependencies are almost identical for the LM with distilled water (Fig. 18) and the time of unsteady CO_2 transfer is about 30 seconds. In case of LM with potassium carbonate theoretical and experimental dependencies show a significant increase in the time of unsteady transfer for highly concentrated solutions up to 800 seconds. This is the result of the CO_2 consumption by a non-saturated potassium carbonate solution during its diffusion through the liquid phase. The more concentrated the solution, the more time is needed for its saturation. Theoretical dependencies in Fig. 19 display faster increase in CO_2 flux as compared to their experimental counterparts. The explanation of this behavior can be the influence of heat effects during CO_2 absorption by non-saturated solution that was not taken into account.

Unsteady transfer of other gases such as N_2, O_2 etc. through LM is very close to one represented in Fig. 18 even at high concentration of potassium carbonate in liquid phase, therefore at initial time effective separation of such components as N_2, O_2 etc. from CO_2 is possible.

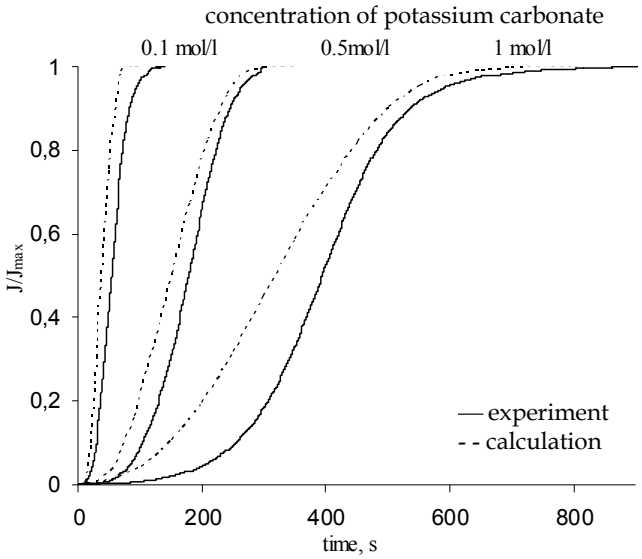

Fig. 19. Unsteady CO_2 transfer through LM with potassium carbonate.

5. Conclusion

As it follows from results of mathematical modeling the application of unsteady mass transfer regimes allows effectively control the selectivity of gas mixture separation by membrane. Particularly, the application of pulse and harmonic oscillations of gas concentration permits to adjust separation process by variation of frequency causing variation of amplitude and phase of the concentration waves passing through a membrane and therefore variation of productivity and selectivity of separation. This technique can provide extremely high separation factors at initial times but unfortunately at low productivity. For O_2/N_2 gas mixture concentration wave method is low effective but for Xe/N_2 and Xe/O_2 good separation can be obtained. The study of unsteady mass transfer is important for development of gas sensors with membrane coating since they have low selectivity and therefore respond to all components of gas mixture. Important task in this case is restoring of initial composition of gas at the registration system inlet and actual function of variation of composition during the time based on the sensor response after membrane. Increasing or decreasing of unsteady selectivity can be controlled by creation of new membrane materials and systems with partial or complete immobilization on functional groups introduced in membrane medium. Suggested mathematical apparatus allows to solve these tasks and to formulate requirements to the system "membrane-gas mixture" for realization of unsteady highly effective gas separation processes.

The development of mathematical apparatus of selective unsteady transfer of gas mixtures through membranes is necessary for development of phenomenological description of dynamics of mass transfer of O_2, N_2 and CO_2 in breathing apparatus of humans and animals for understanding of functioning of live organisms.

6. List of symbols

A	membrane area [m^2] or concentration wave amplitude
C	concentration [$kmol/m^3$]
D	diffusivity [m^2/s]
d	width/half-width of peak
H	thickness of membrane [m]
I	ionic strength of solution [$kg\ ion/m^3$]
J	gas flow rate [kmol/s] or [m^3/s]
j	pulse response function [$kmol/(m^2 \cdot s^2)$]
k	reaction rate constant
K	reaction equilibrium constant
L	length [m]
M	initial concentration of K_2CO_3 in solution [$kmol/m^3$]
m, n	integer number
P	permeability coefficient
p	gas partial pressure [Pa]
q	volume of gas [m^3]
R	formation/consumption rate of a component [$kmol/(m^3 \cdot s)$]
S	solubility [$kmol/(m^3 \cdot Pa)$]
T	temperature [K]
t	time [s]
x	coordinate [m]

Subscripts/Superscribts

∞	infinite dilution
A, B	gas mixture components
d	downstream
liq	liquid phase
mem	membrane phase
SS	steady state
US	unsteady state
u	upstream
W	water

Greek

a	selectivity/separation factor
γ	parameter
Δ	asymmetry parameter
Φ	contributions of a component into permeation flux
φ	phase shift
μ	molar mass [kg/kmol]
ω	frequency

7. References

Baker, R. (2002). Future direction of membrane gas separation technology. *Ind. Eng. Chem. Res.*, Vol.41, pp. 1393-1411

Baker, R. (2004). *Membrane technology and application*, 2nd ed., John Wiley & Sons Ltd., California, USA

Beckman, I.; Shelekhin, A. & Teplyakov, V. (1989). Membrane separation of gas mixture under unsteady state conditions. *DAN USSR*, Vol.308, No.3, pp. 635-637 (In Russian)

Beckman, I.; Shelekhin, A. & Teplyakov, V. (1991). Separation of gas mixtures in unsteady-state conditions. *J. Membrane Sci.,* Vol.55, pp. 283-297

Beckman, I. (1993). Unusual membrane processes: non-steady state regimes, nonhomogeneous and moving membranes, In: *Polymeric Gas Separation membranes*, D.R. Paul & Yu.P. Yampolskii, (Eds.), 301-352, CRC Press, Boca Raton, Florida, USA

Beckman, I.; Zheleznov, A. & Loza, K. (1996). Concentration wave method in diagnostics of inhomogeneity of material structure, *Vestnik MGU, Series 2: Chemistry*, Vol.37, No.2, pp. 173-176 (In Russian)

Cents, A.; Brilman, D. & Versteeg, G. (2005). CO_2 absorption in carbonate/bicarbonate solutions: the Danckwerts-criterion revisited. *Chem. Eng. Sci.,* Vol.60, pp. 5830-5835

Chen, H.; Kovvali, A., Majumdar, S. & Sirkar, K. (1999). Selective CO_2 separation from CO_2-N_2 mixtures by immobilized carbonate-glycerol membranes. *Ind. Eng. Chem. Res.*, Vol.38, pp. 3489-3498

Crank, J. (1975). *The mathematics of diffusion*, Clarendon Press, Oxford, UK

Danckwerts, P. & Sharma, M. (1966). The absorption of carbon dioxide into solutions of alkalis and amines (with some notes on hydrogen sulphide and carbonyl sulphide). *Chem. Eng.*, Vol.44, pp. CE244-CE280

Dindore, V.; Brilman, D. & Versteeg, G. (2005). Modelling of cross-flow membrane contactors: mass transfer with chemical reactions. *J. Membrane Sci.,* Vol.255, pp. 275-289

Hwang, S.-T. & Kammermeyer, K. (1975). *Membranes in Separations*, John Wiley & Sons, New York, USA

Lee, Y.; Noble, R., Yeomb, B., Park, Y. & Lee, K. (2001). Analysis of CO_2 removal by hollow fiber membrane contactors. *J. Membrane Sci.,* Vol.194, No.1, pp. 57-67

Morales-Cabrera, M.; Perez-Cisneros, E. & Ochoa-Tapia J. (2005). An approximate solution for the CO_2 facilitated transport in sodium bicarbonate aqueous solutions. *J. Membrane Sci.,* Vol.256, pp. 98-107

Otto, N. & Quinn, J. (1971). The facilitated transport of carbon dioxide through bicarbonate solutions. *Chem. Eng. Sci.,* Vol.26, pp. 949-961

Paul, D. (1971). Membrane separation of gases using steady cyclic operation. *Ind. Eng. Chem. Process Des. Develop.,* Vol.10, No.3, pp. 375-379

Pohorecki, R. & Kucharski, E. (1991). Desorption with chemical reaction in the system CO_2-aqueous solution of potassium carbonate. *Chem. Eng. J.,* Vol.46, pp. 1-7

Rahimpour, M. & Kashkooli, A. (2004). Enhanced carbon dioxide removal by promoted hot potassium carbonate in a split-flow absorber. *Chem. Eng. and Processing,* Vol.43, pp. 857

Shalygin, M.; Okunev, A., Roizard, D., Favre, E. & Teplyakov, V. (2006). Gas permeability of combined membrane systems with mobile liquid carrier. *Colloid Journal* Vol.68, pp. 566-574 (In Russian)

Suchdeo, S. & Schultz, J. (1974). The permeability of gases through reacting solutions: the carbon dioxide-bicarbonate membrane system. *Chem. Eng. Sci.,* Vol.29, No.1, pp. 13-23

Ward, W. & Robb, W. (1967). Carbon dioxide-oxigen separation: facilitated transport of carbon dioxide across a liquid film. *Science* Vol.156, pp. 1481-1484